Highest Connectivity in a Purely Inorganic 3D Compound Based on Paradodecatungstate-B Clusters: Synthesis and Magnetic Properties

Chun-Jing Zhang, Hai-Jun Pang, and Ya-Guang Chen

Key Laboratory of Polyoxometalates Science of Ministry of Education, College of Chemistry, Northeast Normal University, Changchun 130024, P. R. China

Reprint requests to Dr. Yaguang Chen. E-mail: chenyg146@nenu.edu.cn

Z. Naturforsch. **2009**, *64b,* 809 – 814; received February 11, 2009

A new paradodecatungstate-B compound, $[\{Co(H_2O)_4\}_4(H_4W_{12}O_{42})]\cdot 10H_2O$ (**1**) of the polyoxometalate series has been synthesized and characterized by elemental analysis, IR and UV spectroscopy, TG analysis, and single-crystal X-ray diffraction. Compound **1** exhibits a unique 8-connected three-dimensional (3D) framework with a $(4^2 \cdot 8^{20} \cdot 12^6)$ topology. Moreover, **1** displays antiferromagnetic interactions in the 2 – 300 K temperature range, well reproduced by a simulation procedure.

Key words: Polyoxometalates, Paradodecatungstate-B, Transition Metal, 3D Architecture, Magnetic Properties

Introduction

Polyoxometalates (POMs), transition-metal oxide clusters, have obtained an extensive attention, not only because of their controllable shape and size, their high negative charges, and their oxo-enriched surfaces [1 – 11], but also because of their potential applications in catalysis, electrical conductivity, gas storage, ion exchange, and biological chemistry [12 – 18]. In this field, a brand-new advance is the design and construction of intriguing high-dimensional and highly connected frameworks based on POMs. Currently, a promising approach for designing such frameworks is the use of the surface oxygen atoms of POMs for combinations with different transition metal complexes (TMCs). As a result, a series of high-dimensional and highly connected POM-based hybrid materials have been successfully synthesized [19 – 25]. However, to construct high-dimensional and highly connected purely inorganic POM-based materials without the incorporation of additional organic ligands is still a challenge [26, 27]. This kind of materials is usually stable and insoluble in common organic solvents, which is very advantageous *e. g.* to expand the application of POM-based materials in chemically bulk-modified electrodes [28, 29]. Especially, the assembly of purely inorganic POM-based frameworks offers high potential for the formation of a new type of porous materials which combines the thermodynamic stability of zeolites and mesoporous silicas [30] with the sophistication and versatility of metal-organic frameworks (MOFs) [31 – 33].

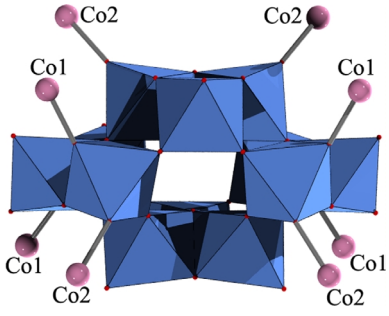

Fig. 1. Combined polyhedral/ball-and-stick view of the coordination environment of the $[H_4W_{12}O_{42}]^{8-}$ anion with attached Co(II) atoms.

In POM chemistry, it is an important rule that the greater the charge density on the surface oxygen atoms of POMs, the more metal ions may coordinate to these units. Compared with well-known POMs, such as Keggin-, Anderson-, Wells-Dawson-, and Lindqvist-type POMs, the paradodecatungstate-B anions possess high charge density and 18 terminal and 18 bridging O atoms, which offer a variety of potential coordination sites to link metal ions and to make the formation of high-dimensional and highly connected frameworks easer. On the other hand, because of the multiple coordination requirements and oxophilicity of transi-

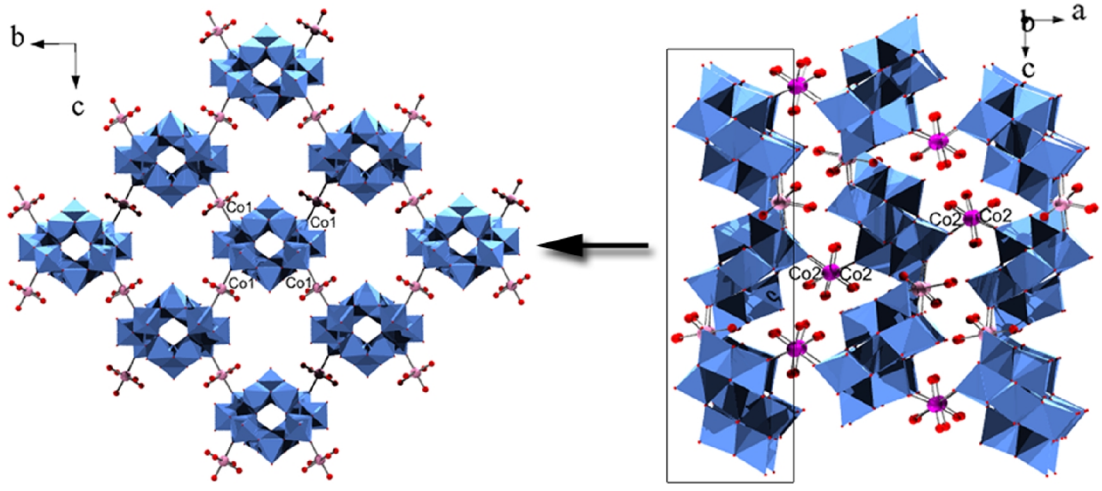

Fig. 2. Combined polyhedral/ball-and-stick view of the 2D layer (left) and the 3D structure (right).

tion metal cations, they are suitable for linking POM units together to form new classes of materials with extended frameworks.

On the basis of the above considerations, we have chosen the paradodecatungstate-B anions as inorganic ligands and Co^{2+} as the transition metal cations to construct highly connected and high-dimensional, purely inorganic materials. Fortunately, we obtained such a compound, $[\{Co(H_2O)_4\}_4(H_4W_{12}O_{42})]\cdot 10H_2O$ (**1**), in which each $[H_4W_{12}O_{42}]^{8-}$ cluster links eight Co^{2+} ions into a 3D framework, displaying the highest connectivity number known to date. In the 3D structure, there are two kinds of channels along the [1 0 0] and [0 0 1] directions, respectively.

Results and Discussion

*Crystal structure of **1***

Single-crystal X-ray diffraction analysis has revealed that **1** consists of protonated paradodecatungstate-B polyanions $[H_4W_{12}O_{42}]^{8-}$, Co atoms and water molecules and exhibits a 3D structure with two kinds of channels. Bond valence sum calculations [34] show that all W and Co atoms are in the +VI and +II oxidation states, respectively. For charge balance, two protons were attached to POMs, which is similar to the cases $\{[Ag(CH_3CN)_2]_4[H_3W_{12}O_{40}]\}$ [27] and $[\{H_2W_{11}Ce(H_2O)_4O_{39}\}_2]\cdot 8H_2O$ [35]. The polyoxoanion is centrosymmetric and consists of four corner-sharing trimers of two types, each of which contains three edge-sharing WO_6 octahedra. In the upper and lower trimer of the $[H_4W_{12}O_{42}]^{8-}$ cluster, the three tungsten atoms define a near-equilateral triangle (angles of 59.85, 59.86, and 60.29°), while the three tungsten atoms in the left or right trimer define an open angle (W_{side}–$W_{central}$–W_{side} = 113.60°). In the triangular trimer, each octahedron has one unshared oxygen atom, while in the open angular trimer each octahedron has two unshared oxygen atoms. According to the type of oxygen atoms bonded to the W atoms, the W–O bond lengths are divided into three categories: 1.714(12) – 1.753(8) Å for W–O(t), 1.801(7) – 2.165(7) Å for W–O(μ^2), and 1.893(7) – 2.283(7) Å for W–O(μ^3) bonds. All these bond lengths are within the normal ranges and in close agreement with those described in the literature [36, 37]. Interestingly, each $[H_4W_{12}O_{42}]^{8-}$ cluster acts as an octadentate ligand coordinating to eight Co^{2+} ions through its terminal oxygen atoms (Fig. 1), which represents the highest connectivity number of the paradodecatungstate-B POMs known to date.

There are two crystallographically unique cobalt atoms with similar coordination environments. Co1 and Co2 are both six-coordinated by two O atoms from two paradodecatungstate-B clusters and four water molecules to form distorted octahedra. The average Co–O bond lengths are 2.084 Å for Co1 and 2.078 Å for Co2. Co1 links two $[H_4W_{12}O_{42}]^{8-}$ clusters, while the $[H_4W_{12}O_{42}]^{8-}$ cluster is surrounded by four $[Co1(H_2O)_4]^{2+}$ bridging cations. Consequently, a 2D layer is formed parallel to the *bc* plane (Fig. 2a). In addition, each $[H_4W_{12}O_{42}]^{8-}$ cluster is surrounded by four $[Co2(H_2O)_4]^{2+}$ cations, and each Co2 ion links two neighboring $[H_4W_{12}O_{42}]^{8-}$

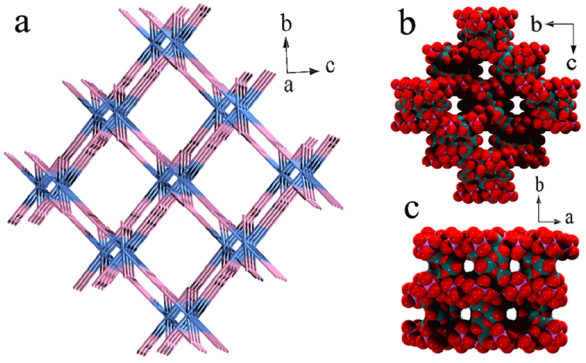

Fig. 3. Schematic view of the 3D structure (a), space-filled representation of the dumbbell-shaped channel along the [1 0 0] direction (b), and the ring-shaped channel along the [0 0 1] direction (c).

clusters belonging to different layers, which extends the 2D layers containing Co1 into a 3D framework along the *b* axis (Fig. 2b). The structure of **1** can be compared to that of similar compounds like $(H_3O^+)_3[\{Na(H_2O)_4\}\{Co(H_2O)_4\}_3(H_2W_{12}O_{42})]\cdot 24.5H_2O$ (**2**) and $[Zn_5(H_2O)_{20}(H_2W_{12}O_{42})]\cdot 6H_2O$ (**3**) reported by the Liu group [38] and the Wang group [39], respectively. Although **2** is a 3D compound, the $[H_2W_{12}O_{42}]^{10-}$ cluster is linked by six CoO_6 octahedra. In **3**, its $[H_2W_{12}O_{42}]^{10-}$ cluster is linked by eight ZnO_6 octahedra, to form a 2D structure. Therefore, **1** represents the highest connectivity and dimensionality for paradodecatungstate-B POM systems.

The 3D structure of **1** can be rationalized as an 8-connected network with $(4^2\cdot 8^{20}\cdot 12^6)$ topology if we assign the -O–Co–O- units as the connectors, and the $[H_4W_{12}O_{42}]^{8-}$ clusters as the 8–connected nodes (Fig. 3a). In the 3D framework, there are two kinds of channels filled with free water molecules: a dumbbell-shaped channel along the [1 0 0] direction and a ring-shaped channel along the [0 0 1] direction, respectively (Fig. 3b and c). Calculations by PLATON have revealed that the van der Waals free space per unit cell (after the solvent-water molecules have been removed) is approximately 2022.3 Å^3, corresponding to 31.3 % of the unit cell volume.

A notable feature of the structure of **1** is that two terminal oxygen atoms linking Co1 and Co2 come from the same WO_6 octahedron of the angular open trimer with the Co–Co distance at 5.858 Å and the Co–W–Co angle at 105.08°. Such a structural motif of paradodecatungstate-B POMs is suitable to build highly connected architectures and can contribute to the magnetic properties of **1**.

UV spectrum and thermal analysis

The UV spectrum of compound **1** is displayed in Fig. 4. It shows two bands (λ = 206 and 263 nm) assigned to $p_\pi(\mathrm{Od}) \rightarrow d_\pi^*(\mathrm{W})$ transitions in the W=O bonds and d_π-p_π-d_π transitions between the energy levels of the tricentric W–O–W bonds, respectively.

The TG analysis was carried out for **1** (Fig. 5) under N_2 atmosphere with a heating rate of 10 °C min^{-1} in the temperature range of 60 – 600 °C. The curve shows two weight loss steps: The first continuous weight loss step below 450 °C corresponds to the loss of crystal water and coordinated water 11.8 % (calcd. 13.1 %). The second weight loss step of 1.1 % (calcd. 1.0 %) in the range of 450 – 600 °C is ascribed to the release

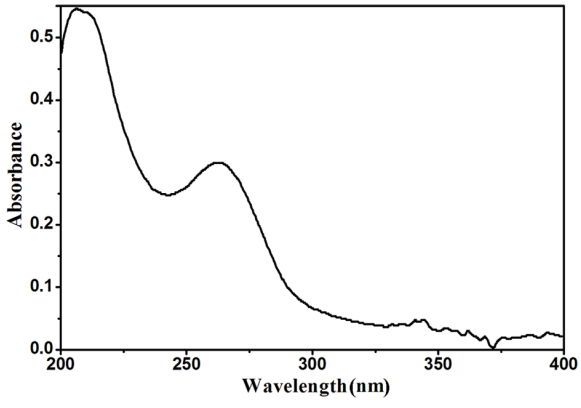

Fig. 4. The UV spectrum of compound **1**.

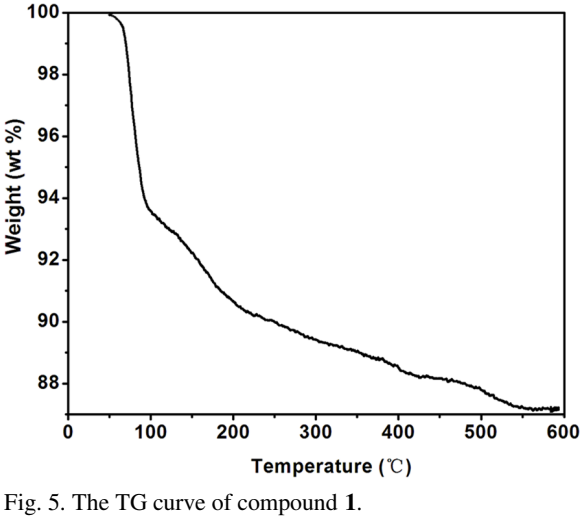

Fig. 5. The TG curve of compound **1**.

of two H_2O molecules, according to the decomposition reaction

$$Co_4[H_4W_{12}O_{42}] \rightarrow 4\,CoO + 12\,WO_3 + 2H_2O$$

The total weight-loss (12.8 %) for **1** is consistent with the calculated value (13.6 %). It is notable that the temperature required for the loss of water molecules of **1** is 450 °C, which is higher than that of other systems [38, 39], perhaps caused by the higher connectivity and dimensionality of the title compound.

Magnetic properties

The solid-state magnetic behavior of **1** has been investigated. The variable-temperature magnetic susceptibility was measured in the temperature range of 2–300 K at a fixed field strength of 1000 O_e and plotted as $\chi_m T$ and $\chi_m{}^{-1}$ *versus* T, as shown in Fig. 6. The $\chi_m T$ value of **1** slowly decreases from 10.17 $cm^3{\cdot}K{\cdot}mol^{-1}$ at 300 K to 5.57 $cm^3{\cdot}K{\cdot}mol^{-1}$ at 2 K, which in principle reveals paramagnetic behavior. The $\chi_m T$ product at 300 K is higher than the spin-only value (g = 2.0) of 7.75 $cm^3{\cdot}K{\cdot}mol^{-1}$ for four non-interacting Co^{2+} ions (S = 3/2) probably due to the contribution of an orbital angular momentum at high temperature [40]. The $\chi_m{}^{-1}$ *versus* T plot is almost linear in the range of 50–300 K, closely following the Curie-Weiss law, giving a Curie constant C = 10.9 $cm^3{\cdot}K{\cdot}mol^{-1}$ and a Weiss constant Θ = −22.5 K. The Weiss constant indicates that in **1** there exist weak antiferromagnetic interactions. On the basis of the connection modes of the Co(II) ions to the polyoxoanion in **1**, the Co atoms (Co1 and Co2) connected to the WO_6 octahedron are considered as a Co_2 unit, and the others are described as isolated atoms

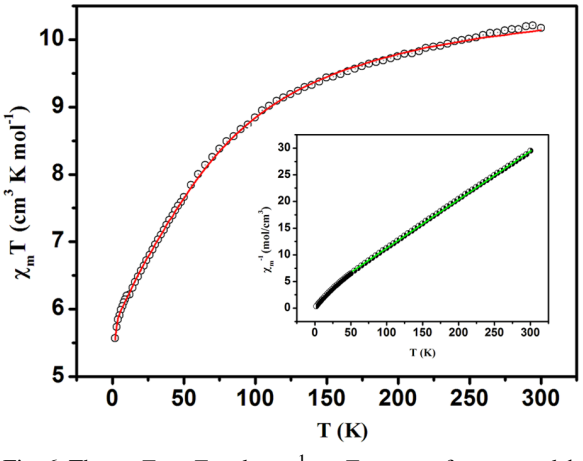

Fig. 6. The $\chi_m T$ *vs.* T and $\chi_m{}^{-1}$ *vs.* T curves of compound **1**.

(see Fig. 1). The susceptibility was simulated according to a model of dimeric $[Co(II)]_2$ plus two isolated Co(II) metal ions (S = 3/2) with the isotropic Heisenberg spin Hamiltonian for the dimer of

$$H = -2\,J\,S_1\,S_2 \quad (1)$$

where S_i is the spin operator for each metal ion (S_i = 3/2 for Co(II) with i = 1 to 2) and J is the magnetic interaction in the nuclear unit. The magnetic data of **1** are fitted to the following equation, where N, g, β, and k have their usual meanings

$$\chi_{dimer} = \frac{2Ng^2\beta^2}{kT}\,\frac{e^{2J/kT}+5e^{6J/kT}+14e^{12J/kT}}{1+3e^{2J/kT}+5e^{6J/kT}+7e^{12J/kT}} \quad (2)$$

$$\chi_m = \chi_{dimer} + 2\frac{Ng^2\beta^2}{3kT}S(S+1) \quad (3)$$

This simulation procedure works well over the whole temperature range (see the line in Fig. 6) with the parameters g = 3.40 and J = −12.55 cm^{-1}. The negative J value further confirms that there is a weak antiferromagnetic interaction between the Co(II) centers. The theoretical expressions for **1** not only indicate the occurrence of weak coupling interactions between the metal ions through a -O–W–O- bridge but also support the structure of **1**.

Conclusions

In summary, a new extended solid framework composed of transition metal cations (M = Co^{2+}) and paradodecatungstate-B clusters has been obtained and characterized. In this compound, paratungstate clusters serve as eight-dentate ligands and link the metal ions into high-dimensional structures. The magnetic studies of compound **1** indicate that there exist weak antiferromagnetic interactions. The isolation of compound **1** shows that paradodecatungstate-B clusters are good inorganic ligands for designing highly connected and high-dimensional structures with specific properties.

Experimental Section

General procedures

All reagents were commercially available and were used without further purification. $Na_{10}[H_2W_{12}O_{42}]{\cdot}20H_2O$ was synthesized according to the literature [41] and characterized by IR and UV spectroscopy, and TG analysis. Elemental analyses (Co and W) were carried out with a Leaman inductively coupled plasma (ICP) spectrometer. The IR spectrum (KBr pellets) was recorded on a Nicolet 170SX FT-IR

Table 1. Crystal data and structure refinement parameters for **1**.

Empirical formula	$H_{52}Co_4O_{68}W_{12}$
M_r	3582.22
Crystal system	orthorhombic
Space group	*Pnma*
a, Å	18.720(6)
b, Å	19.687(6)
c, Å	17.509(5)
V, Å^3	6453.0(3)
Z	4
D_{calcd}, g cm^{-3}	3.7
μ(MoK_α), mm^{-1}	22.4
T, K	293(2)
F(000), e	6368.0
θ range for data collection, deg	1.90 – 25.75
Reflections collected/unique	34121/6366
R_{int}	0.0434
Data / parameters	6366 / 376
$R1/wR2$ [$I \geq 2\sigma(I)$]	0.0293/0.0878
$R1/wR2$[a] (all data)	0.0358/0.0912
GOF[b] (F^2)	1.052
Largest diff. peak/hole, e Å^{-3}	3.15/−1.79

[a] $R1 = \|\|F_o| - |F_c\|/\Sigma|F_o|$; [b] $wR2 = [\Sigma w(F_o^2 - F_c^2)^2/\Sigma w(F_o^2)^2]^{1/2}$, $w = [\sigma^2(F_o^2) + (0.0553P)^2 + 50.09P]^{-1}$, where $P = (\mathrm{Max}(F_o^2, 0) + 2F_c^2)/3$, GoF = $[\Sigma w(F_o^2 - F_c^2)^2/(n_{obs} - n_{param})]^{1/2}$.

spectrophotometer in the range 400 – 4000 cm^{-1}. The UV spectrum was recorded in the range of 200 – 400 nm in aqueous solution on a DU-70 spectrophotometer. TG analysis was recorded with a Netzsch STA 449C microanalyzer in an atmosphere of nitrogen at a heating rate of 10 °C min^{-1}. Variable temperature magnetic susceptibility measurements were carried out on a Quantum Design MPMS-5SQUID magnetometer with an applied field of 1000 O_e. Diamagnetic correction was estimated from Pascal's constants.

*Preparation of [{Co(H$_2$O)$_4$}$_4$(H$_4$W$_{12}$O$_{42}$)]·10H$_2$O (**1**)*

Freshly prepared $Na_{10}[H_2W_{12}O_{42}]\cdot 20H_2O$ (0.3470 g, 0.1 mmol) was first suspended in 20 mL of distilled water, to which a solution of $Co(CH_3COO)_2\cdot 2H_2O$ (0.0747 g, 0.3 mmol) was added dropwise with stirring. The initial pH of the mixture was carefully adjusted to 5.1 with 1 M HCl and NaOH solution. The mixture was heated for 1 h at 80 °C and allowed to cool to r. t. Then a minor precipitate was filtered off. The filtrate was left to evaporate slowly under ambient conditions. After ten days, pink crystals were isolated in about 38 % yield (based on W). Anal. for $H_{52}Co_4O_{68}W_{12}$: calcd. Co 6.58, W 61.58; found Co 6.76, W 62.88. – IR (KBr): ν = 3439(vs), 1632(s), 946(s), 872(m), 716(m), 561(w), 489(m), 405(m) cm^{-1}.

Table 2. Selected bond lengths (Å) and bond angles (deg) for compound **1**[a].

Co(1)-O(3)	1.990(8)	Co(1)-O(8)	2.008(8)
Co(1)-O(8W)	2.101(10)	Co(1)-O(9W)	2.112(9)
Co(1)-O(7W)	2.136(9)	Co(1)-O(6W)	2.156(9)
Co(2)-O(3W)	2.048(10)	Co(2)-O(18)$^{\#3}$	2.058(8)
Co(2)-O(11)	2.071(8)	Co(2)-O(4W)	2.080(10)
Co(2)-O(5W)	2.104(10)	Co(2)-O(10W)	2.106(12)
O(3)-Co(1)-O(8)	176.2(3)	O(3)-Co(1)-O(8W)	87.5(4)
O(8)-Co(1)-O(8W)	91.7(4)	O(3)-Co(1)-O(9W)	88.7(4)
O(8)-Co(1)-O(9W)	92.2(4)	O(8W)-Co(1)-O(9W)	176.1(4)
O(3)-Co(1)-O(7W)	91.7(3)	O(8)-Co(1)-O(7W)	92.0(3)
O(8W)-Co(1)-O(7W)	90.0(4)	O(9W)-Co(1)-O(7W)	89.5(4)
O(3)-Co(1)-O(6W)	91.0(4)	O(8)-Co(1)-O(6W)	85.3(4)
O(8W)-Co(1)-O(6W)	93.5(5)	O(9W)-Co(1)-O(6W)	87.2(4)
O(7W)-Co(1)-O(6W)	175.7(4)	O(3W)-Co(2)-O(18)$^{\#3}$	179.2(5)
O(3W)-Co(2)-O(11)	84.4(4)	O(18)$^{\#3}$-Co(2)-O(11)	95.4(3)
O(3W)-Co(2)-O(4W)	91.2(5)	O(18)$^{\#3}$-Co(2)-O(4W)	88.1(4)
O(11)-Co(2)-O(4W)	90.0(4)	O(3W)-Co(2)-O(5W)	89.6(4)
O(18)$^{\#3}$-Co(2)-O(5W)	90.6(4)	O(11)-Co(2)-O(5W)	173.7(4)
O(4W)-Co(2)-O(5W)	92.2(5)	O(3W)-Co(2)-O(10W)	94.9(6)
O(18)$^{\#3}$-Co(2)-O(10W)	85.9(4)	O(11)-Co(2)-O(10W)	89.9(4)
O(4W)-Co(2)-O(10W)	173.9(5)	O(5W)-Co(2)-O(10W)	88.5(5)

[a] Symmetry transformation used to generate equivalent atoms: $^{\#3}$ $x - 1/2, y, -z + 1/2$.

X-Ray crystallography

X-Ray diffraction data were collected on a SMART CCD diffractometer with graphite-monochromatized MoK_α radiation at r. t. The structure was solved with Direct Methods and refined with full-matrix least-squares on F^2 with the SHELX-97 program package [42]. The non-hydrogen atoms were located with difference Fourier syntheses. The crystallographic data are listed in Table 1, and selected bond lengths and bond angles are presented in Table 2.

Further details of the crystal structure investigation may be obtained from Fachinformationszentrum Karlsruhe, 76344 Eggenstein-Leopoldshafen, Germany (fax: +49-7247-808-666; e-mail: crysdata@fiz-karlsruhe.de, http://www.fiz-informationsdienste.de/en/DB/icsd/depot_anforderung.html) on quoting the deposition number CSD-419938.

Acknowledgement

This work was supported by the Analysis and Testing Foundation of the Northeast Normal University.

[1] M. T. Pope, *Heteropoly and Isopoly Oxometalates*, Springer, Berlin, **1983**.
[2] J. S. Anderson, *Nature* **1937**, *140*, 850.
[3] C. L. Hill *Chem. Rev*. **1998**, *98*, 1
[4] Y. Wei, B. Xu, C. L. Barnes, Z. Peng, *J. Am. Chem. Soc*. **2001**, *123*, 4083.
[5] L. C. W. Baker, D. C. Glick, *Chem. Rev*. **1998**, *98*, 3.
[6] A. Müller, S. Q. N. Shah, H. Bögge, M. Schmidtmann, *Nature* **1999**, *397*, 48.
[7] K. Fukaya, T. Yamase, *Angew. Chem*. **2003**, *115*, 678; *Angew. Chem. Int. Ed*. **2003**, *42*, 654.
[8] E. Coronado, C. J. Gómez-García, *Chem. Rev*. **1998**, *98*, 273.
[9] C. Z. Lu, C. D. Wu, H. H. Zhuang, J. S. Huang, *Chem. Mater*. **2002**, *14*, 2649.
[10] Q. Li, Y. Wei, J. Hao, Y. Zhu, L. Wang, *J. Am. Chem. Soc*. **2007**, *129*, 5810.
[11] D. L. Long, E. Burkholder, L. Cronin, *Chem. Soc. Rev*. **2007**, *36*, 105.
[12] H. Y. An, E. B. Wang, D. R. Xiao, Y. G. Li, Z. M. Su, L. Xu, *Angew. Chem*. **2006**, *118*, 918; *Angew. Chem. Int. Ed*. **2006**, *45*, 904.
[13] M. Wei, C. He, W. Hua, C. Duan, S. Li, Q. Meng, *J. Am. Chem. Soc*. **2006**, *128*, 13318.
[14] K. Uehara, H. Nakao, R. Kawamoto, S. Hikichi, N. Mizuno, *Inorg. Chem*. **2006**, *45*, 9448.
[15] Y. Ishii, Y. Takenaka, K. Konishi, *Angew. Chem*. **2004**, *116*, 2756; *Angew. Chem. Int. Ed*. **2004**, *43*, 2702.
[16] J. M. Knaust, C. Inman, S. W. Keller, *Chem. Commun*. **2004**, 492.
[17] R. Kawamoto, S. Uchida, N. Mizuno, *J. Am. Chem. Soc*. **2005**, *127*, 10560.
[18] W. Ninomiya, M. Sadakane, S. Matsuoka, H. Nakamura, H. Naitou, W. Ueda, *Chem. Commun*. **2008**, 5239.
[19] R. L. LaDuca, Jr., R. S. Rarig, Jr., J. Zubieta, *Inorg. Chem*. **2001**, *40*, 607.
[20] P. J. Hagrman, J. Zubieta, *Inorg. Chem*. **2001**, *40*, 2800.
[21] C. J. Zhang, Y. G. Chen, H. J. Pang, D. M. Shi, M. X. Hu, J. Li, *Inorg. Chem. Commun*. **2008**, *11*, 765.
[22] Y. P. Ren, X. J. Kong, X. Y. Hu, M. Sun, L. S. Long, *Inorg. Chem*. **2006**, *45*, 4016.
[23] J. Y. Niu, P. T. Ma, H.. Niu, J. Li, J. W. Zhao, Y. Song, J. P. Wang, *Chem. Eur. J*. **2007**, *13*, 8739.
[24] J. Q. Sha, J. Peng, H. S. Liu, J. Chen, A. X. Tian, P. P. Zhang, *Inorg. Chem*. **2007**, *46*, 11183.
[25] A. X. Tian, J. Ying, J. Peng, J. Q. Sha, Z. G. Han, J. F. Ma, Z. M. Su, N. H. Hu, H. Q. Jia, *Inorg. Chem*. **2008**, *47*, 3274.
[26] H. Q. Tan, Y. G. Li, Z. M. Zhang, C. Qin, X. L. Wang, E. B. Wang, Z. M. Su, *J. Am. Chem. Soc*. **2007**, *129*, 10066.
[27] C. Streb, C. Ritchie, D. L. Long, P. Kögerler, L. Cronin, *Angew. Chem*. **2007**, *119*, 7723; *Angew. Chem. Int. Ed*. **2007**, *46*, 7579.
[28] K. Kalcber, *Electroanalysis* **1990**, *2*, 419.
[29] X. L. Wang, E. B. Wang, Y. Lan, C. W. Hu, *Electroanalysis* **2002**, *14*, 1116.
[30] H. van Bekkum, J. Cejka (Eds.), *Zeolites and ordered mesoporous materials: Progress and prospects. Studies in Surface Science*, Vol. 157, Elsevier, Amsterdam, The Netherlands, **2005**.
[31] M. Eddaoudi, D. B. Moler, H. Li, B. Chen, T. M. Reineke, M. O'Keeffe, O. M. Yaghi, *Acc. Chem. Res*. **2001**, *34*, 319.
[32] S. L. James, *Chem. Soc. Rev*. **2003**, *32*, 276.
[33] H. Li, M. Eddaoudi, M. O'Keeffe, O. M. Yaghi, *Nature* **1999**, *402*, 276.
[34] I. D. Brown, D. Altermatt, *Acta Crystallogr*. **1985**, *B41*, 244.
[35] H. J. Pang, C. J. Zhang, D. M. Shi, Y. G. Chen, *Cryst. Growth. Des*. **2008**, *8*, 4476.
[36] H. T. Evans, Jr., E. Prince, *J. Am. Chem. Soc*. **1983**, *105*, 4838.
[37] X. T. Zhang, D. Q. Wang, J. M. Dou, S. S. Yan, X. X. Yao, J. Z. Jiang, *Inorg. Chem*. **2006**, *45*, 10629.
[38] C. Y. Sun, S. X. Liu, L. H. Xie, C. L. Wang, B. Gao, C. D. Zhang, Z. M. Su, J. *Solid State Chem*. **2006**, *179*, 2093.
[39] L. Yuan, C, Qin, X. L. Wang, E. B. Wang, Y. G. Li, *Solid State Sci*. **2008**, *10*, 967
[40] O. Kahn, *Molecular Magnetism*, VCH, Weinheim **1993**.
[41] H. T. Evans, Jr., O. W. Rollins, *Acta. Crystallogr. Sect. B* **1976**, *32*, 1565.
[42] G. M. Sheldrick, SHELXS/L-97, Programs for Crystal Structure Determination, University of Göttingen, Göttingen (Germany) **1997**; see also: G. M. Sheldrick, *Acta Crystallogr*. **2008**, *A64*, 112.